Supplemental information
Ultrathin Liquid Sheets: Water Gets in Shape for VUV Absorption

Jonas Knurr,[a] Patrick Hemberger,[a] Patrick Ascher,[a] Sven Augustin,[a] David J. Hoffman,[c] Gregor Knopp,[a] Samuel Menzi,[a] Zhibin Sun,[a] Simon Tiefenbacher,[a] Reto Wetter,[a] Jake D. Koralek,[c] Antoine Sarracini,[a] Kirsten Schnorr,[a] Christoph Bostedt,[a,b] Andras Bodi,[a] Andre Al Haddad[a]

[a] *Paul Scherrer Institut, CH-5232, Villigen PSI, Switzerland*

[b] *LUXS Laboratory for Ultrafast X-ray Sciences, Institute of Chemical Sciences and Engineering, École Polytechnique Fédérale de Lausanne (EPFL), CH-1015, Lausanne, Switzerland*

[c] *SLAC National Accelerator Laboratory, Menlo Park, CA, 94025, USA*

S1. MICROFLUIDIC LIQUID JET INTERFACE

The microfluidic chip features two inlets, one for the liquid sample and the other for the squeezing gas. The liquid channel, with a diameter of 20 µm, is centered in the chip, while the gas inlet was split into two channels with a diameter of 50 µm each. The gas channels intercept the liquid channel outlet at an angle of ±40° relative to the fluid channel. Adjusting the liquid and gas flow rates allows the sheet thickness and size to be precisely and reproducibly controlled. A polyether ether ketone (PEEK) holder was designed to interface the chip with IDEX tubing. Fluorocarbon (FKM) O-rings between the holder and the glass chip ensured a leak-free seal.

Control of liquid flow rates in the range of 0.1–1 ml · min^{-1}, requiring pressures up to 40 bar, was achieved using a Shimadzu LC-20AD HPLC pump. Helium served as the squeezing gas, and its flow rate was regulated by an MKS mass flow controller between 80–200 sccm using backing pressures of up to 6 bar.

S2. EXPERIMENTAL CHAMBER AND DETECTION SYSTEM

The setup was based on a windowless absorption experiment for gaseous samples[1] and integrated into a compact, differentially pumped vacuum system depicted in Fig. SI 1. The liquid sheet is housed in a central absorption vacuum chamber separated from the beamline gas filter and the detector chamber by two skimmers. An upstream chamber served as a mounting point for a 1 mm diameter entrance skimmer and was pressurized with approximately 15 mbar of helium. Opposite the entrance skimmer, the smaller detector skimmer was installed to shield the photodiode detector and act as an exit slit defining the photon energy and the probe area on the liquid sheet. The detector skimmer featured a 100 µm diameter aperture, and the detector chamber was pressurized with 5 mbar of helium. This arrangement ensured a unidirectional helium flow from the gas filter and detector chambers toward the absorption chamber, preventing vapor migration from the interaction region toward the gas filter or detector.

A photodiode (OptoDiode SXUV100) was employed as the detector to measure the transmitted photon intensity. The photocurrent was read out with a Keithley 6485 Picoammeter. The diode and skimmer were mounted on a three-axis manipulator, allowing alignment with the incoming beam and adjusting the distance between the skimmers. The distance between the skimmers during the operation was typically 2 mm.

From the top, a combined, three-axis linear and rotary manipulator allowed the positioning of the liquid sheet intercepting the VUV beam. The four-axis manipulator enabled both the translation and rotation of the liquid sheet, facilitating the interception of the beam at various locations along its surface and, consequently, the modulation of the probed thickness. Also, this system allowed the displacement of the liquid sheet away from the beam trajectory for background measurements and to assess the contribution of the vapor phase to the measured extinction.

Opposite the liquid sheet inlet, a liquid nitrogen-cooled trap was mounted. The trap was approximately 50 cm long, which, together with the flight path in the absorption cell and through the T-piece, provided sufficient room for the jet stream to break up into droplets before impacting on the cold metal surface. The piece served a dual purpose: as a catcher to store the liquid and as a cryogenic pump condensing the vapor in the chamber. It was crucial for preventing the rapid build-up of icicles. The interaction regions were pumped with an ACP 120 G Roots pump via a 40 mm VAT diaphragm valve to control the pumping speed. The pressure was monitored with a Pirani gauge. During operational conditions, the pressure of the interaction chamber was maintained at 0.3 mbar, dominated by the He squeezing gas. Two viewports on the experimental chamber allowed illumination and optical monitoring of the liquid sheet and observation of interaction volume between the skimmers.

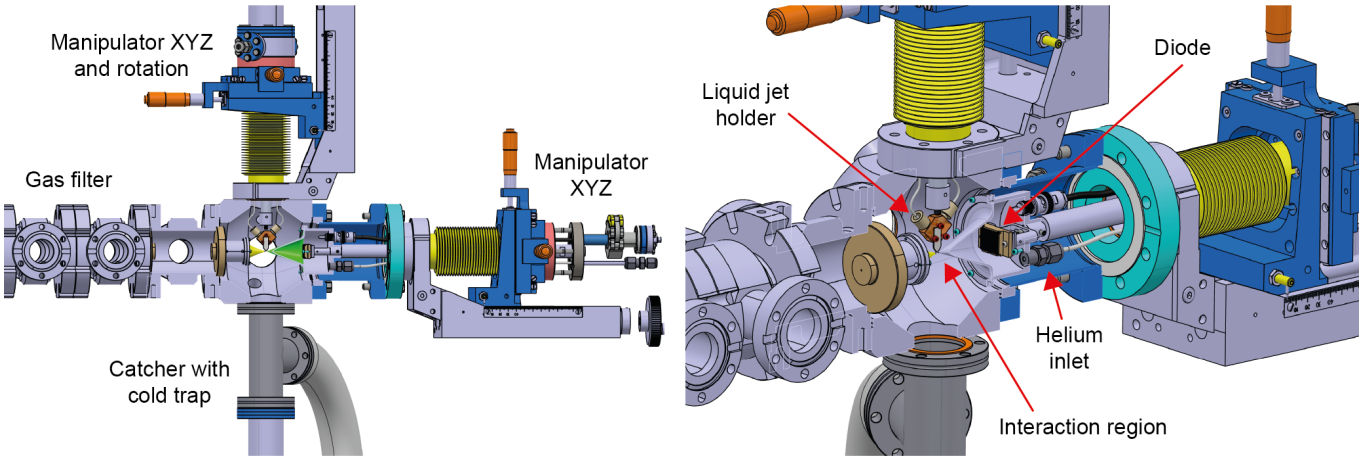

FIG. SI 1. Experimental setup. (Left) The VUV beam propagates from left to right, passing through the differential pumping stages of the gas filter (only the last two stages are shown). The beam is focused into the interaction chamber, passing through the sample target. A photodiode detector is mounted directly into the beam path to measure the photon flux. (Right) Main interaction chamber. An entrance skimmer with a local pressure higher than in the interaction chamber and the gas filter chamber is used to flush the interaction volume with helium and reduce the water vapor column density in the light path, as well as to ensure that sample vapor does not diffuse into the gas filter chamber. The exit skimmer towards the detector allows the detector volume to be filled with overpressure helium to stop sample vapor from diffusing downstream toward the diode. The exit skimmer also serves as the defining aperture for the probe area.

S3. EXPERIMENTAL PROCEDURES

At the beginning of the experiment, the skimmers were aligned and centered on the VUV beam trajectory using the visible white light of the grating, which follows the same beam path as the monochromatized VUV beam. Next, the chamber was pumped to transport the VUV beam to the interaction region. The detector chamber was then positioned to the maximum transmission of the VUV. The PEEK holder of the liquid sheet was moved into the beam path. The VUV beam footprint could be estimated with the microscope based on the visible fluorescent emission of PEEK. This also served as a reference point for positioning the liquid sheet relative to the beam.

The sheet was positioned at the focus of the beamline. However, in the vertical direction, in which the monochromator disperses the light, the sheet is practically fully illuminated through the 1 mm aperture of the entrance skimmer. Horizontally, the approximately 500 µm focus is wider than the sheet, meaning the VUV beam illuminated the whole liquid sheet. To set the sheet thickness over the sampling region and as an exit slit for energy selection, the detector skimmer with an opening diameter of 100 µm acted as defining aperture for sampling.

The liquid sheet was started at atmospheric pressure with moderate liquid and helium flow rates of 0.2 ml $\cdot$ min^{-1} and 80 sccm for a reliable start-up. Subsequently, the chamber was pumped down gradually until it reached base pressure. Then, the trap was cooled with liquid nitrogen to freeze the liquid in the catcher and help condense water vapor in the chamber. This procedure ensured a controlled and reproducible start of the liquid sheet. After stabilizing vacuum and jet conditions, the liquid sheet position was adjusted for optimal intersection with the VUV beam.

Based on the previously determined vertical beam position, the liquid sheet could be moved directly to the correct height. Subsequently, the sheet was aligned at the center between the skimmers, defining its position along the beam propagation axis. To optimize the third axis across the VUV beam, the photon energy was set to 8.5 eV, where water exhibits a peak in the absorption cross section. Then, a systematic scanning of the liquid sheet position across the VUV beam was performed while monitoring the transmitted beam through the photodiode response. Knowing the sheet contour, adjustments were made to position the VUV beam at the center between the two edges.

[1] A. Bodi, J. Knurr, P. Ascher, P. Hemberger, C. Bostedt and A. Al Haddad, *J. Synchrotron Rad.*, 2024, **31**, 1257–1263.